Journal of Applied Physics

Delocalization of vortex in $SmBa_2Cu_3O_{7-\#}$ superconducting films with $BaHfO_3$ nano-rods

Cite as: J. Appl. Phys. **120**, 103902 (2016); https://doi.org/10.1063/1.4962398
Submitted: 06 June 2016 . Accepted: 26 August 2016 . Published Online: 13 September 2016

Yuji Tsuchiya, Satoshi Awaji, Kazuo Watanabe, Shun Miura, Yusuke Ichino, Yutaka Yoshida, and Kaname Matsumoto

Delocalization of vortex in $SmBa_2Cu_3O_{7-\delta}$ superconducting films with $BaHfO_3$ nano-rods

Yuji Tsuchiya,[1,2] Satoshi Awaji,[1] Kazuo Watanabe,[1] Shun Miura,[2] Yusuke Ichino,[2] Yutaka Yoshida,[2] and Kaname Matsumoto[3]
[1]*High Field Laboratory for Superconducting Materials, Institute for Materials Research, Tohoku University, Sendai 980-8577, Japan*
[2]*Department of Energy Engineering and Science, Nagoya University, Nagoya 464-8603, Japan*
[3]*Department of Materials Science and Engineering, Kyushu Institute of Technology, Kitakyushu 804-8550, Japan*

(Received 6 June 2016; accepted 26 August 2016; published online 13 September 2016)

Transport measurements revealed flux pinning properties and vortex phases in $SmBa_2Cu_3O_{7-\delta}$ (Sm123) superconducting films with $BaHfO_3$ nano-rods on $LaAlO_3$ substrates. The films have large matching fields B_Φ up to 9.9 T, nano-rod diameters of ~6 nm, and a slight T_c degradation with $T_c \sim 91.8$ K by using the low temperature growth technique. According to the transport results, a small critical exponent ~4 indicates the presence of a Bose-glass phase in the films. Double peaks of the flux pinning force density are unexpectedly observed at high temperatures over 80 K, which is accompanied by steep drops of the crossover magnetic fields between the single vortex pinning and the collective pinning states. The drops are explained by the delocalization of the vortex where the vortex is pinned by many nano-rods in the single vortex pinning state. From the viewpoint of the vortex delocalization, we conclude that B_Φ should be less than 11 T for applications at liquid nitrogen temperature. *Published by AIP Publishing*. [http://dx.doi.org/10.1063/1.4962398]

INTRODUCTION

Rare-earth cuprate high temperature superconductors $REBa_2Cu_3O_y$ (RE123, *RE*: rare earth elements including Y) have a high critical temperature T_c over 90 K. They possess a large critical current density J_c at high magnetic fields and temperatures. Therefore, the RE123 tape is a promising conductor to be used for various kinds of large-scale electric devices such as high field magnets[1–3] and the other applications.[4] However, J_c and the irreversible magnetic field B_{irr} rapidly decrease with increasing operation temperature. Therefore, the optimization of J_c is necessary for the RE123 tapes to be used at various temperatures above the liquid helium temperature: the liquid nitrogen of 65–77 K, the liquid hydrogen of 20 K, or at the cryocooler as 4.2–40 K. Another problem of the RE123 tape is the large angular dependence of J_c for the applied magnetic field direction because the RE123 is a highly anisotropic material.[5] To overcome these problems, introduction of the artificial pinning centers (APCs) into the RE123 films has been extensively studied. For example, the pillar shaped nano-rod or the sphere shaped nano-dot is introduced as APCs. Among APCs, the nano-rod effectively enhances J_c at a high temperature.[6] There are several ways to introduce nano-rods into the RE123 films. Since 1990s, the heavy ion irradiation is a major technique to introduce correlated defects as pinning centers into the RE123 films.[7] However, the particle irradiation suppresses T_c; therefore, it is not adequate for discussion on the effect of the nano-rods. In 2004, MacManus has reported a new method to introduce the nano-rods into the RE123 films by modifying the film deposition process.[6] It improves the J_c anisotropy. Following the report, some manufacturers adopted the process-based APC introduction for commercial RE123 tapes. To achieve improvements of the pinning by the nano-rods, Tobita has reported that the $BaHfO_3$ (BHO) nano-rods effectively improve J_c at high temperature in Gd123 films.[8] Very recently, Miura has reported that the Sm123 films with the BHO nano-rods grown with the low temperature growth technique (LTG) have a small T_c degradation.[9] The LTG method can introduce highly dense nano-rods into the RE123 films with small T_c degradation. Therefore, the RE123 films with nano-rods made by the latest technique are good candidates to discuss the vortex physics and the vortex pinning at high temperature because the T_c is robust for changing the density of the nano-rods. In this work, we investigate vortex pinning phases in the nano-rod introduced RE123 films with tiny T_c degradation at various temperatures and magnetic fields. We also discuss the optimization of J_c based on the vortex phase, especially concerning about the vortex delocalization.

EXPERIMENTAL METHOD

BHO nano-rod doped Sm123 films were deposited on $LaAlO_3$ (LAO) single crystal substrates with (100) surface by the LTG technique.[9] The films were deposited by using the pulse laser deposition (PLD) method and the alternating target method with Sm123 and BHO targets. To confine the narrow nano-rods, the Sm123 seed layer without nano-rods was deposited on the LAO substrate at 870°. Then, the BHO nano-rod doped Sm123 upper layer was grown at 750° on the seed layer of thickness about 50 nm. The thickness of the films is about 350 nm including the seed layer. The contents of the BHO, determined by the ICP mass spectroscopy, are 1.6 vol. % and 5.6 vol. %. We refer to these samples as low density (LD, $T_c = 91.8$ K) and high density (HD, $T_c = 91.0$ K)

samples, respectively. After the deposition, the film was processed into a micro-bridge with a width of 100 μm and a length of 1 mm using a YAG laser etching with a metal mask. The critical current density J_c and the resistivity ρ were measured at various temperatures and magnetic fields between 20–100 K and 0–17 T by the four-probe transport method using a probe with a sample rotator at HFLSM in Tohoku Univ. J_c is determined for an electric field criterion of 1 μV/cm. The magnetic field is applied perpendicular to the films corresponding to the direction along the c-axis of the Sm123 matrix. After the transport measurements, the shape and the number density of the nano-rods are observed by using a transmission electron microscope (TEM) apparatus.

RESULTS AND DISCUSSION

Figure 1 shows the TEM images of the LD and HD samples. According to the plan-view images (not shown), the LD and HD samples have matching fields of 2 T and 9.9 T, respectively. The diameter of the nano-rods is ~6 nm in both samples as shown in the inset of Fig. 1. The nano-rods are aligned in the HD sample slightly more than in the LD because of the repulsive interaction between the nano-rods during the growth process.

Field dependence of J_c at various temperatures in the BHO doped Sm123 films is shown in Fig. 2. At low temperature, the J_c is robust below the matching fields B_Φ. And the J_c rapidly decreases above B_Φ. At higher temperatures, J_c starts to drop at lower magnetic field less than B_Φ. The enhancement of J_c near B_Φ disappears above 88.5 K and 86 K in the LD sample and the HD sample, respectively. In this high temperature region, the J_c-B exponent $\alpha = d(\log J_c)/d(\log B)$ is below -1, which is explained by the collective vortex pinning phase even at low magnetic fields. It indicates that the nano-rods are not so effective very close to T_c. In the HD sample, the B_{irr} is 15.4 T at 77 K, which is a relatively high value, compared with the reports about that in RE123 films with nano-rods. We define the crossover magnetic field B^* between the single vortex pinning and the collective pinning as the field with $\alpha = -0.5$. The reference line for $\alpha = -0.5$ is drawn as the dashed line in Fig. 2. Then, we estimate the crossover magnetic field B^* as the field with $\alpha = -0.5$.

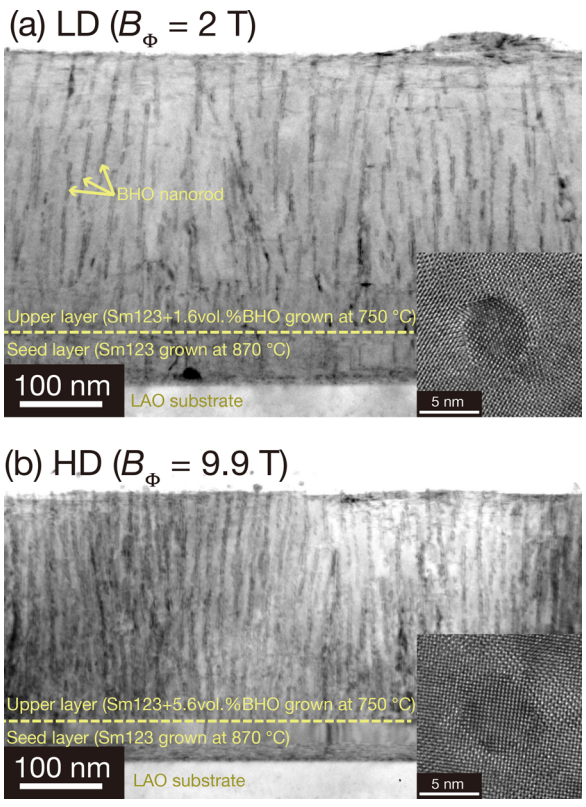

FIG. 1. TEM images of the Sm123 films with (a) 1.6 vol. % and (b) 5.6 vol. % BHO contents.

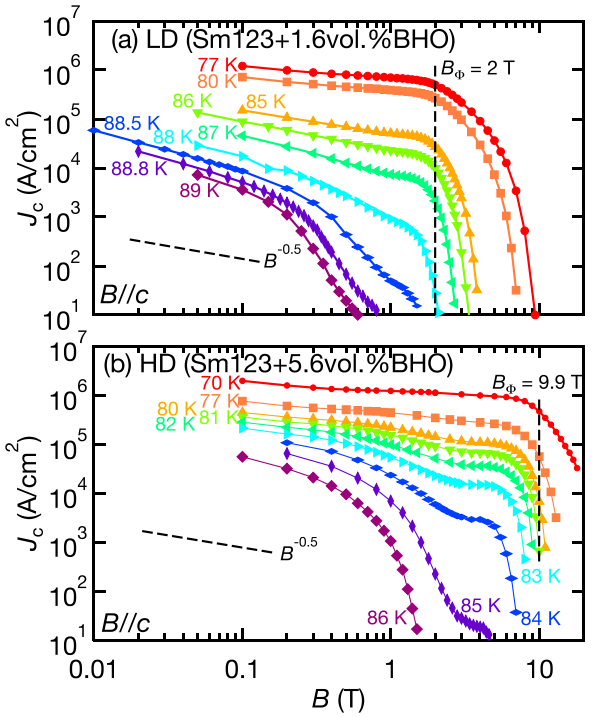

FIG. 2. Field dependences of J_c in the (a) LD and (b) HD samples at various temperatures with $B//c$.

The pinning force density F_p values in the LD and HD samples were calculated as $F_p = J_c \times B$, and the field dependence of normalized F_p at each temperature is plotted in Fig. 3. It is obvious that the peak magnetic field B_p approaches B_Φ at low temperatures. At high temperatures near 80 K, unexpected two peaks of F_p appear. The origin of the double peaks is discussed later based on the vortex pinning phase diagram. From the field dependences, higher peak field B_p^{high} and low peak field B_p^{low} are estimated. The double peak structure appears over several Kelvin in both samples. The minimum temperature for the double peak appearance is 86 and 80 K in the LD sample and the HD sample, respectively.

We now discuss the vortex phase. The critical exponent of the vortex liquid-glass transition is calculated from the temperature dependences of the resistivity ρ. The temperature dependences are fitted with the linear curve in the parameter of $(d\log\rho/dT)^{-1}$. As a result, the critical exponent s is as small as ~4 at fields less than the B_Φ as shown in Fig. 4. It indicates that the Bose-glass state possibly appears in this system.[10–12] In the following, we discuss the vortex pinning states concerning the Bose-glass phase.

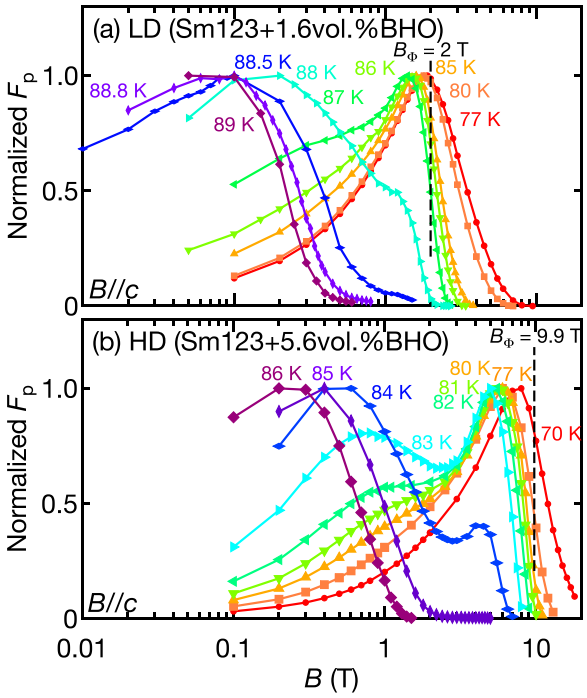

FIG. 3. Field dependences of normalized F_p in the (a) LD and (b) HD samples at various temperatures.

To sum up the transport results, the magnetic field vs. temperature diagrams are shown in Figs. 5(a) and 5(b) for the LD and HD samples, respectively. The inset figures show the same diagrams for wider temperature ranges. In the figures, red circles show the irreversible fields B_{irr}, the orange hollow circles show the liquid-glass transition line B_g, the blue squares show the peak fields of the pinning force density B_p^{high} for the higher peak and B_p^{low} for the lower peak, and the green triangles show the crossover field B^* between the single vortex pinning and the collective pinning regime. As reported in the RE123 films with the nano-rods, the temperature dependence of irreversible field has a shoulder at a high temperature.[13] The liquid-glass transition line follows the irreversibility line. Just below the upturn temperature of

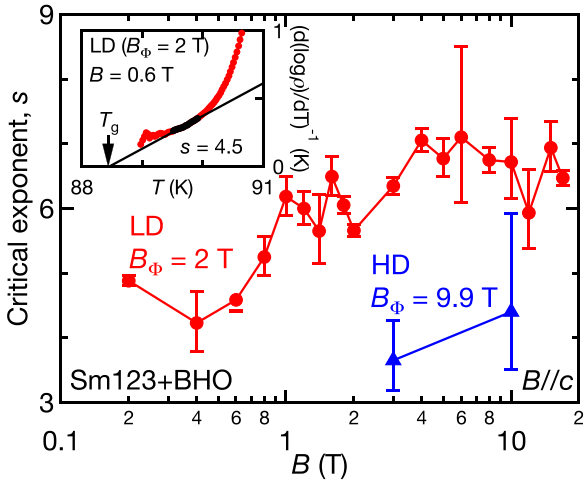

FIG. 4. Field dependences of the critical exponent s in the LD and HD samples. The inset shows a typical fitting result to estimate the critical exponent s.

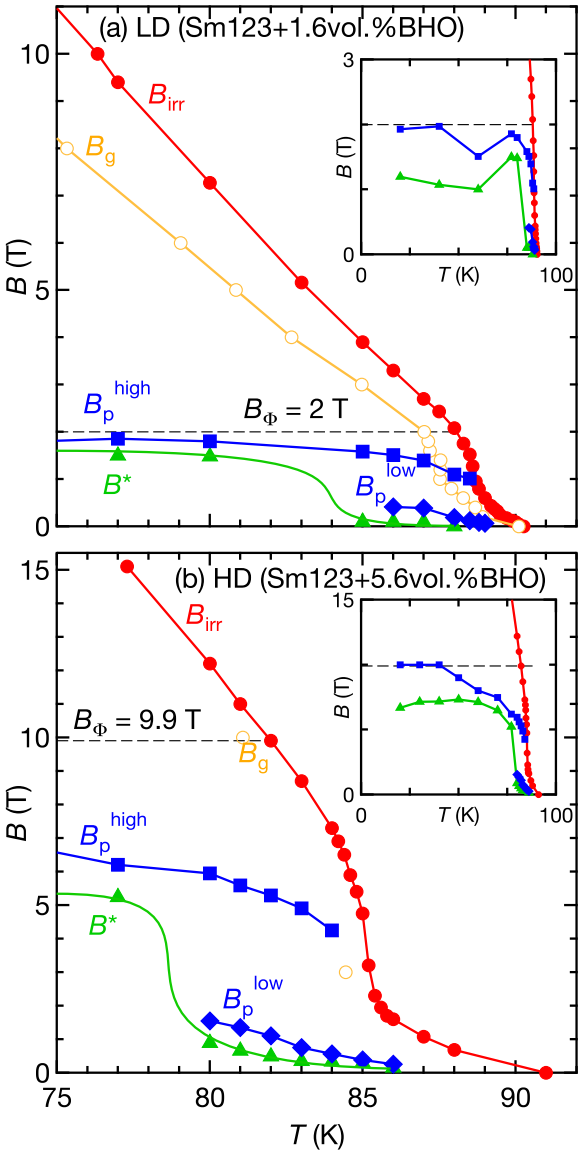

FIG. 5. Phase diagrams of vortex phase for the (a) LD and (b) HD samples. The irreversible line (red circles) and glass transition line (orange hollow circles), peak field B_p (blue squares), and crossover field B^* (green triangles) are shown in lines.

the irreversibility line, the higher peak B_p^{high} for the pinning force appears at almost half of the matching fields in both samples. On the other hand, the lower peak B_p^{low} exists even above the upturn temperatures. Both the peaks become larger at lower temperatures. At certain temperatures, the B_p^{low} disappears in both samples. The crossover field B^* is located near the minimum of B_p^{high} or B_p^{low} at each temperature. B^* follows B_p^{low} above 85 K and 80 K in the LD and HD samples, respectively. It suddenly grows up to B_p^{high} at the lower temperature. In the following, we focus on the sudden jump of the B^* at 77–80 K for the LD sample and at 80–85 K for the HD sample because B^* is an important parameter to describe the feasible field range with the single vortex pinning without the large degradation of J_c in the magnetic field.

Figure 6 shows the schematic diagrams of vortex pinning phases to explain the experimental results in this study

based on the Blatter's theory.[12] There are two characteristic temperatures where the vortex pinning efficiency changes. $T_{r\xi}$ is the temperature where the vortex size is equal to the nano-rod size ($\sqrt{2}\xi(T) = r_r$, where r_r is the radius of the nano-rods), and it is estimated as 62 K using $r_r = 3$ nm and the coherence length of $\xi(0\,\mathrm{K}) = 1.2$ nm. Then, the efficiency of the nano-rods becomes weak above $T_{r\xi}$, resulting in the smaller crossover field than the matching field. T_{dl} is the delocalization temperature where the mean amplitude of the thermal fluctuation becomes equal to the distance between the nano-rods. This transition is explained as the 2D-Boson analogy that the vortex as the Bose particle can move from one pinning center to the other by thermal fluctuation. Above T_{dl}, the vortex cannot be pinned by the individual nano-rods; therefore, the vortex is pinned by many nano-rods in the single vortex pinning regime. The interaction length between vortices increases because of the delocalization and the winding of the vortex; the crossover field B^* rapidly decreases with increasing temperature above T_{dl}. With the small B^*, J_c largely decreases even under a small magnetic field because the power-law exponent of field dependent J_c becomes large in the collective vortex pinning regime. From the phase diagrams, it becomes clear that B^* becomes larger with the more dense nano-rods; however, T_{dl} shifts to lower temperatures. The higher B^* and the higher T_{dl} are better for the application of the RE123 tapes under the magnetic field, and then they are in tradeoff. T_{dl} in the Sm123 + BHO nano-rod system is estimated by using the 2D-Boson theory later.

In the experimental diagrams, B_p^{high} coexists with B_p^{low} at higher temperatures just above T_{dl}. This behavior has never been predicted and observed.[12] B_p^{high} is explained as the extended effective matching field. On the other hand, there are two possible origins of B_p^{low}: the effective matching field of the vortex pinned by many nano-rods or the peak field for the random pinning centers. At such a high temperature, the small random pinning centers are negligible compared with the large correlated pinning centers. Therefore, the former scenario is preferable. Other possible origin is not the enhanced pinning force but the reduction of the pinning by the double kink excitation of the vortices.[14,15] The vortex delocalization provides the easier hopping between nano-rods, resulting in the rapid vortex creep. As an additional evidence, current-voltage exponent, n-value, has a plateau at the magnetic field with the minimum F_p (not shown). For a more detailed discussion, the other measurement technique at the different electric field range is required such as the magnetic relaxation. Above all, it is important that some evidences support the vortex delocalization presence at high temperatures. Here, we do not concentrate on discussion on the double peak structure but on the delocalization of the vortex at T_{dl}.

T_{dl} is calculated by an equation[12] as

$$\frac{T_{dl}}{T_c} \approx \frac{r_r}{2\sqrt{2}\pi\xi(0)\sqrt{Gi}}\left(1-\frac{T_{dl}}{T_c}\right)1n\left[\frac{d_r^2}{2\xi^2(0)}\left(1-\frac{T_{dl}}{T_c}\right)\right], \quad (1)$$

where r_r is 3 nm, $\xi(0)$ is the coherence length at 0 K as 1.2 nm, Gi is the Ginzburg-number as 0.01, and d_r is the mean distance between the nano-rods as $\sqrt{\Phi_0/B_\Phi}$. From the equation, T_{dl} is estimated as 84 K and 78 K for the LD ($B_\Phi = 2$ T) and HD ($B_\Phi = 10$ T) samples, respectively. These estimated temperatures are in good agreement with the temperatures where the B^* jumps as shown in Fig. 5. Finally, the B_Φ dependence of T_{dl} is shown in Fig. 7, with the T_c data for the various doping levels in the films with the LTG technique. The doping level dependence of the T_c assumed as the parabolic curve was taken into account. As a result, T_{dl} decreases almost linearly with increasing the doping levels in a vast doping region. As a rough formulation, T_{dl} is simplified as T_{dl} (K) = 85–0.7 (K/T)* B_Φ (T) in this system. The red error bars indicate the T_{dl} estimated from the experimental results. The experimental results match well with the calculated result.

Finally, we discuss the effective way to enhance J_c at high temperature under magnetic fields. From this study, it was clarified that the delocalization of the vortex accelerates the crossover from the single vortex to the collective pinning state, and the delocalization temperature can be controlled by the doping level of the nano-rods which corresponds to the change of the distance between the nano-rods. From the B_Φ dependence of the T_{dl}, $B_\Phi \sim 11$ T is the best matching

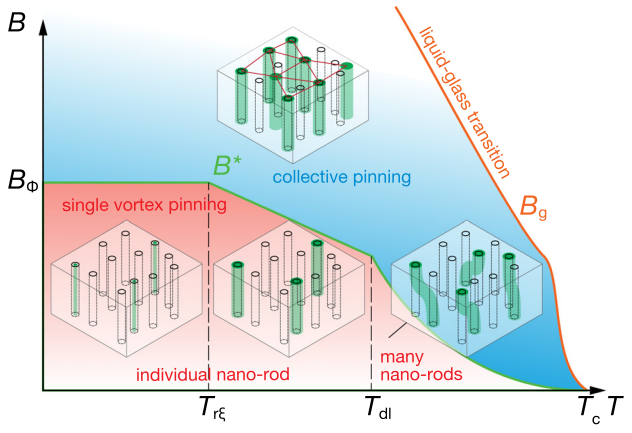

FIG. 6. Schematic phase diagram of the vortex in the correlated pinning regime on the basis of Ref. 12.

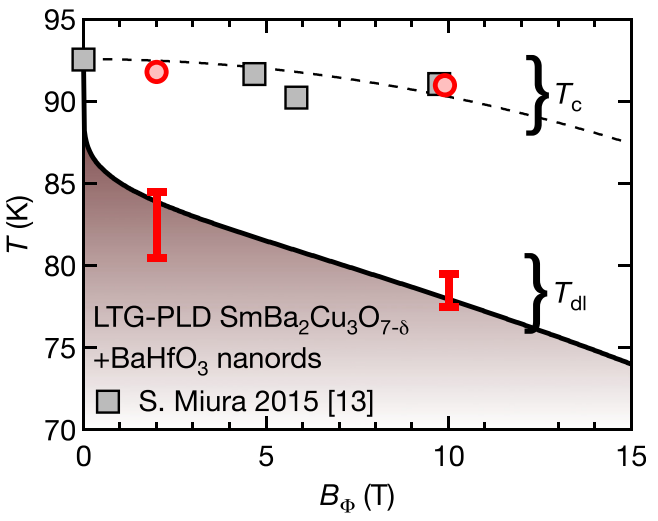

FIG. 7. The matching field dependence of the delocalization temperature in BHO doped Sm123 films.

field for the application of the RE123 tapes under magnetic field at liquid nitrogen temperature.

CONCLUSIONS

Flux pinning properties and vortex phases in $SmBa_2Cu_3O_7$ superconducting films with $BaHfO_3$ nano-rods made by the LTG method are studied by transport measurements. Two kinds of films were prepared with matching fields of 2 T (LD sample) and 9.9 T (HD sample) with a slight T_c degradation. As a result, the small critical exponent $\sim$4 under a magnetic field less than the matching field indicates the possible appearance of the Bose-glass phase in the films. The delocalization of the vortex, where the individual vortex is pinned by many nano-rods in the single vortex pinning state, was observed at 80–85 K and 77–80 K in the LD and HD samples in association with the steep drop of the crossover magnetic field between the single vortex pinning and the collective pinning phases. The delocalization temperatures agree with the theoretical estimation based on the 2D-Boss glass theory. Unexpectedly, double peaks of the pinning force density are observed at 85–88 K and 80–84 K just above the delocalization temperature in the LD and HD samples, respectively. At last, the effective nano-rod doping level in this system is discussed as less than 11 T for the application at the liquid nitrogen temperature.

ACKNOWLEDGMENTS

This work was partially supported by the JST-ALCA, JSPS Grant in Aid (10324659, 25246032, 26889005, and 16K20898). The transport results are measured at the HFLSM, IMR in Tohoku University. The TEM images are taken by Mr. Shun Ito at the Analytical Research Core for Advanced Materials, IMR, Tohoku University.

[1]S. Awaji, K. Watanabe, H. Oguro, S. Hanai, H. Miyazaki, M. Takahashi, S. Ioka, M. Sugimoto, H. Tsubouchi, S. Fujita, M. Daibo, Y. Iijima, and H. Kumakura, IEEE Trans. Appl. Supercond. **24**, 4302005 (2014).
[2]H. W. Weijers, W. D. Markiewicz, A. J. Voran, S. R. Gundlach, W. R. Sheppard, B. Jarvis, Z. L. Johnson, P. D. Noyes, J. Lu, H. Kandel, H. Bai, A. V. Gavrilin, Y. L. Viouchkov, D. C. Larbalestier, and D. V. Abraimov, IEEE Trans. Appl. Supercond. **24**, 4301805 (2014).
[3]S. Yoon, J. Kim, H. Lee, S. Hahn, and S.-H. Moon, Supercond. Sci. Technol. **29**, 04LT04 (2016).
[4]L. Rossi, A. Badel, M. Bajko, A. Ballarino, L. Bottura, M. M. J. Dhalle, M. Durante, P. Fazilleau, J. Fleiter, W. Goldacker, E. Haro, A. Kario, G. Kirby, C. Lorin, J. van Nugteren, G. de Rijk, T. Salmi, C. Senatore, A. Stenvall, P. Tixador, A. Usoskin, G. Volpini, Y. Yang, and N. Zangenberg, IEEE Trans. Appl. Supercond. **25**, 4001007 (2015).
[5]U. Welp, W. K. Kwok, G. W. Crabtree, K. G. Vandervoort, and J. Z. Liu, Phys. Rev. Lett. **62**, 1908 (1989).
[6]J. L. MacManus-Driscoll, S. R. Foltyn, Q. X. Jia, H. Wang, A. Serquis, L. Civale, B. Maiorov, M. E. Hawley, M. P. Maley, and D. E. Peterson, Nat. Mater. **3**, 439 (2004).
[7]J. C. Barbour, E. L. Venturini, and D. S. Ginley, Nucl. Instrum. Methods Phys. Res. **65**, 531 (1992).
[8]H. Tobita, K. Notoh, K. Higashikawa, M. Inoue, T. Kiss, T. Kato, T. Hirayama, M. Yoshizumi, T. Izumi, and Y. Shiohara, Supercond. Sci. Technol. **25**, 062002 (2012).
[9]S. Miura, Y. Yoshida, Y. Ichino, A. Tsuruta, K. Matsumoto, A. Ichinose, and S. Awaji, Jpn. J. Appl. Phys., Part 1 **53**, 090304 (2014).
[10]D. R. Nelson and V. M. Vinokur, Phys. Rev. B **48**, 13060 (1993).
[11]D. R. Nelson and V. M. Vinokur, Phys. Rev. Lett. **68**, 2398 (1992).
[12]G. Blatter, V. B. Geshkenbein, A. I. Larkin, and V. M. Vinokur, Rev. Mod. Phys. **66**, 1125 (1994).
[13]S. Miura, Y. Yoshida, Y. Ichino, A. Tsuruta, K. Matsumoto, A. Ichinose, and S. Awaji, Supercond. Sci. Technol. **28**, 114006 (2015).
[14]B. Maiorov, S. A. Baily, H. Zhou, O. Ugurlu, J. A. Kennison, P. C. Dowden, T. G. Holesinger, S. R. Foltyn, and L. Civale, Nat. Mater. **8**, 398 (2009).
[15]L. Miu, Phys. Rev. B **85**, 104519 (2012).